



Published in final edited form as:

*Glycoconj J.* 2006 November ; 23(0): 555–563. doi:10.1007/s10719-006-7668-1.

## Isolation and characterization of heparan sulfate from various murine tissues

**Mohamad Warda,**

Department of Biochemistry- Faculty of Veterinary Medicine, Cairo University

**Toshihiko Toida,**

Faculty of Pharmaceutical Sciences, Chiba University

**Fuming Zhang,**

Biotechnology Center and Departments of Chemistry and Chemical Biology, Chemical and Biological Engineering and Biology, Rensselaer Polytechnic Institute

**Peilong Sun,**

College of Biological and Environmental Engineering, Zhejiang University of Technology

**Eva Munoz,**

Biotechnology Center and Departments of Chemistry and Chemical Biology, Chemical and Biological Engineering and Biology, Rensselaer Polytechnic Institute

**Jin Xie, and**

Biotechnology Center and Departments of Chemistry and Chemical Biology, Chemical and Biological Engineering and Biology, Rensselaer Polytechnic Institute

**Robert J. Linhardt**

Biotechnology Center and Departments of Chemistry and Chemical Biology, Chemical and Biological Engineering and Biology, Rensselaer Polytechnic Institute

Robert J. Linhardt: linhar@rpi.edu

### Abstract

Heparan sulfate (HS), is a proteoglycan (PG) found both in the extracellular matrix and on cell surface. It may represent one of the most biologically important glycoconjugates, playing an essential role in a variety of different events at molecular level. The publication of the mouse genome, and the intensive investigations aimed at understanding the proteome it encodes, has motivated us to initiate studies in mouse glycomics focused on HS. The current study is aimed at determining the quantitative and qualitative organ distribution of HS in mice. HS from brain, eyes, heart, lung, liver, kidney, spleen, intestine and skin was purified from 6–8 week old male and female mice. The recovered yield of HS from these organs is compared with the recovered whole body yield of HS. Structural characterization of the resulting HS relied on disaccharide analysis and  $^1\text{H-NMR}$  spectroscopy. Different organs revealed a characteristic HS structure. These data begin to provide a structural understanding of the role of HS in cell-cell interactions, cell signaling

and sub-cellular protein trafficking as well as a fundamental understanding of certain aspects of protein-carbohydrate interactions.

## Keywords

Heparan sulfate; Glycomics; Glycome; Glycosaminoglycans

---

## Introduction

The cell surface is richly decorated in glycosaminoglycans (GAGs) attached to the core proteins of proteoglycans (PGs). GAGs protect large regions of protein surface from proteases and promote cellular interactions with proteins and other cells [1]. Heparan sulfate (HS), one of the major cell surface carbohydrate determinants, is important in cellular communication in the extracellular matrix that controls physiological pathophysiological events. HS has been isolated from a wide variety of animals ranging from *C. elegans* and *D. melanogaster* to humans [2–6]. Structural differences have been demonstrated for HS isolated from a given organ derived from different species [7,8] for different organ systems within a single species [9–13] and in the same organ system at different developmental stages [5]. Moreover, HSPGs can undergo structural changes during progressive pathological events [12,14]. These differences suggest structural and functional diversity of this important class of glycoconjugates across organs, species, developmental stages and disease states. Structural diversity of HS is initially generated during HS biosynthesis in the Golgi by sequential modifications to the heparosan precursor, initially comprised of alternating *N*-acetyl- $\alpha$ -D-glucosamine 1 $\rightarrow$ 4 linked to  $\beta$ -D-glucuronic acid. These modifications involve enzymes including *N*-deacetylase/*N*-sulfotransferase, glucuronyl *C*-5 epimerase and HS-2-*O*-, 6-*O*- and 3-*O*-sulfotransferases [15]. Several of these enzymes occur in multiple isoforms having different specificity and are expressed in a time-dependent and tissue-dependent fashion [16]. Moreover, the control and regulation of the action of these enzymes within the Golgi, result in the biosynthesis of specific binding sites (*i.e.*, the antithrombin III binding site) [17] and domains (*i.e.*, S-domains) [18], remains unclear. Although recent advances in the cloning and recombinant expression of these various enzymes have begun to illuminate specific sequence requirements for these isoforms [19], the real products of HS biosynthesis found *in vivo* remain poorly understood. In a recent study, the structure of heparan sulfate in control and genetically modified mice was examined [13]. This study did not examine gender differences in the amount or chemical structure of the heparan sulfate isolated from each tissue nor did it assess the presence or amount of iduronic acid in mouse organs.

The current study describes the first systematic effort to examine the yield and distribution of HS across different organ systems of both genders of a single animal species, ICR strain mice. Structural characterization by disaccharide analysis and NMR spectroscopy is described.

## Material and methods

### Materials

Chondroitin ABC lyase (EC 4.2.2.4) from *Proteus vulgaris*, endonuclease (EC 3.1.30.2) from *Serratia marcescens* (Sigma Chemicals, St. Louis, MO), actinase E (Kaken Pharmaceutical Co. Ltd., Tokyo) and heparin lyase I (heparinase EC 4.2.2.7), heparin lyase II (heparitinase II), heparin lyase III (heparitinase I EC 4.2.2.8) from *Flavobacterium heparinum* (Seikagaku Biochemicals, Tokyo) were used in these studies. Spectra/Por<sup>®</sup> dialysis tubing MWCO3500 was from Spectrum Medical Industries, Inc. (Los Angeles, CA). Heparin and HS, obtained from porcine intestine, were from Celsus Laboratories Inc. (Cincinnati Ohio). Bovine kidney HS, cetylpyridinium chloride tetra-*n*-butylammonium hydrogen sulfate and 2-cyanoacetamide were purchased from Sigma. Unsaturated disaccharides from HS and heparan sulfate (from bovine kidney) were purchased from Sigma. Perchloric acid (70% v/v), chloroform, methanol, sodium borohydride were from Fischer Chemical Co. (Fairlawn, NJ) All other reagents used were analytical grade. ICR male and female mice of 4–6 weeks old were used in this study. More than 150 animals of each gender were used. Animals were killed by decapitation. The eyes and brain are collected from the head. Heart and lung are taken from thorax, liver, spleen, kidney, small intestine are collected from the abdomen. Whole liver lobes were loosened from surrounding tissue, the tissue was cut at the insertion of blood vessels into hepatic hilus to gain all the tissue possible. Lung was collected at the bifurcation of the trachea into the 2 bronchi. The heart collected by cutting from its base with the major blood vessels attached. Both kidneys were separated from the body with their connected renal vessels and ureters just on emerging from renal hillus. The whole brain was collected from the cranial cavity including the medulla oblongata at its connection with the cervical spinal cord. Small intestine from duodenum to the end of the ileum was separated without the attached mesentery or omental fat. Spleens are freed from surrounding mesentery and cut intact out of the body. The intact eyes are pulled out from orbital cavity with small attached part of the optical nerve (less than 1 mm long). The skins were also collected. Harvested organs were weighed and immediately frozen then kept in  $-40^{\circ}\text{C}$  until processing.

### Tissues processing, isolation and purification of heparan sulfate

Organs were cut into small pieces (<1 mm) and crushed with dry ice into very fine homogenized powder using a mortar and pestle. Fat was removed by washing the powdered tissues with chloroform/methanol mixtures (2:1, 1: 1, 1: 2 (v/v)). The defatted materials were dried under vacuum and stored at  $-40^{\circ}\text{C}$  until further use. The dried, defatted tissues were each suspended in 0.05 M Tris acetate buffer (pH 8.0) and digested for 48 h by actinase E (10 mg/g) at  $50^{\circ}\text{C}$ . The proteolyzed homogenates were placed in a boiling water bath for 15 min to deactivate the protease and then centrifuged ( $2500 \times g$ ) for 30 min at  $4^{\circ}\text{C}$ . The recovered supernatant was next  $\beta$ -eliminated (modified method from [20]) using sodium borohydride (1% w/v) under mild alkaline conditions (0.2M NaOH at  $4^{\circ}\text{C}$  overnight). After neutralization (with 0.2 M HCl) perchloric acid (75%) was added to obtain a final concentration of 5% v/v. Precipitated protein was removed by centrifugation ( $10,000 \times g$  for 30 min at  $4^{\circ}\text{C}$ ) and the supernatant was recovered, dialyzed in cellulose membrane tubing (molecular weight cut-off (MWCO) 3500) against distilled water for 2 successive days at

4°C. The retentate was recovered, cetylpyridinium chloride (CPC) was added (0.1% w/v), the mixture was allowed to stand for 3 h at 4°C, centrifugation was performed ( $2500 \times g$ ) at 4°C for 15 min, the precipitate was recovered, keep washed 2 times with 0.1 % CPC solution. Finally, the recovered precipitate was dissolved in 2.5M NaCl and the crude GAG was recovered by methanol (85% v/v) precipitation. After standing overnight at 4°C the crude GAG precipitate was recovered by centrifugation ( $2500 \times g$ ) at 4°C for 15 min, dialyzed (3500 MWCO) and freeze-dried.

Crude GAGs (0.5–10 mg according to their origin) were treated with chondroitin lyase ABC (2 m unit/mg in 50 mM sodium acetate, pH 8) at 37°C for 24 h in sealed tubes to remove all traces of galactosaminoglycans. The action of the enzyme was confirmed using chondroitin sulfate A. After chondroitinase digestion, the reactions were terminated by heating in a boiling water bath for 5 min and the digested samples were desalted using a Sephadex G-10 microanalysis desalting spin column (Harvard Apparatus Inc. MA, USA) and freeze-dried. Next the freeze-dried sample (0.3–5 mg) was dissolved in 20 mM Tris-HCl buffer (pH 8) containing 2 mM magnesium chloride and digested with endonuclease (2500 m units/mg) for 12 h at 37°C [21] to remove any nucleic acid contaminants. After endonuclease digestion, the reactions were terminated by heating in boiling water bath for 5 min and the samples were desalted using a Sephadex G-10 microanalysis desalting spin columns and the resulting purified HS samples were freeze-dried.

### Chemical characterization using $^1\text{H-NMR}$ analysis

NMR spectroscopy was performed on the purified HS samples dissolved in  $^2\text{H}_2\text{O}$  (99.96 atom %), filtered through a 0.45  $\mu\text{m}$  syringe filter (Millipore Corporation, MA, USA), freeze-dried twice from  $^2\text{H}_2\text{O}$  to remove exchangeable protons and transferred to Shigemi tubes. One dimensional (1D)  $^1\text{H-NMR}$  experiments were performed on a Bruker DRX-400 equipped with NMR Nuts (PC computer) processing and plotting software. On some samples 2D NMR was also performed.

### Enzymatic depolymerization of glycosaminoglycans

The purified HS samples were next treated with heparinase lyases I, II, III to perform disaccharide analysis [22]. Dried samples were dissolved in buffer (50 mM sodium phosphate buffer, pH 7.1 and 100 mM NaCl) each at a concentration of 20  $\mu\text{g}/\text{ml}$ . Each heparin lyase was added at 0, 8 and 16 h to a final concentration of 1 mIU/ $\mu\text{l}$  GAG dry weight. The reaction mixture was incubated on membrane of Ultrafree<sup>®</sup>-MC centrifugal filter spin DEAE membrane column (5000 nominal molecular weight limit) (NMWL), Amicon Millipore Corp., Bedford, MA, USA) at 37°C over a period of 24 h. The disaccharides were recovered from the spin column by centrifugation (12000 rpm) for 30 min at 4°C. The disaccharide products were freeze-dried prior to disaccharide analysis.

### Determination of unsaturated disaccharides from HS

Unsaturated disaccharides produced enzymatically from heparan sulfate were determined by a reversed-phase ionpair chromatography with ultra-sensitive and specific post-column fluorescence detection [23]. The chromatographic equipment included a gradient pump (L-7000), a chromato-integrator (D-7500) from Hitachi Instruments (San Jose, CA), a double

plunger pump for the reagent solution (AA-100-S, Eldex Laboratories, Napa, CA), a sample injector with a 20- $\mu$ l loop (model 7125, Reodyne, Rohnert Park, CA), a fluorescence spectrophotometer (RF-10A<sub>XL</sub>, Shimadzu Scientific, Columbia, MD), a column heater (CH-30), a dry reaction bath (FH-40), and a thermocontroller (TC-55) from Brinkman Instruments (Westbury, NY). A gradient was applied at a flow rate of 1.1 ml/min on a Senshu Pak Docosil (4.6  $\times$  150 mm) at 55°C. The eluents used were as follows: A, H<sub>2</sub>O; B, 0.2M sodium chloride; C, 10 mM tetra-*n*-butylammonium hydrogen sulfate; D, 50% acetonitrile. The gradient program was as follows: 0–10 min, 1–4% eluent B; 10–11 min, 4–15% eluent B; 11–20 min, 15–25% eluent B; 20–22 min, 25–53% eluent B; 22–29 min, 53% eluent B; equilibration with 1% B for 20 min. The proportions of eluent C and D were constant at 12 and 17%, respectively. To the effluent were added aqueous 0.5% (w/v) 2-cyanoacetamide solution and 0.25 M sodium hydroxide at the same flow rate of 0.35 ml/min by using a double plunger pump. The mixture passed through a reaction coil (internal diameter, 0.5 mm; length, 10 m) set in a dry reaction temperature controlled bath at 125°C and a following cooling coil (internal diameter, 0.25 mm; length, 3 m). The effluent was monitored fluorometrically (excitation, 346 nm; emission, 410 nm).

## Results

### HS yield from different organs

The total HS recovered from different organs of male and female mice are presented in Table 1. These data represent an average yield based on more than 150 animals for each gender. The isolation process was performed on two independent batches (each using ~75 animals per gender). The reproducibility of the isolation method is very high with a variation of only 5–10% (depending on the organ) between the two batches. The weight of female mice was only 73% of male mice, so many of the female organs were similarly smaller than their male counterparts. Organs, such as the brain and eyes, were of comparable weight in both genders. The total whole body HS yield as a function of dry defatted weight differed little between male and female animals. Interestingly, female mouse liver and kidney showed a higher HS level than the same organs in male mice. In contrast, the yield of HS from male mice brain was much higher than that obtained from female mouse brain.

### HS disaccharide composition

An established highly reproducible and sensitive HPLC method was used for the analysis of unsaturated disaccharides HS [23] (Figure 1). The lower limit of detection for HS was approximately 0.5–1.5 ng and all results were performed in duplicate.

The mole percentage of each disaccharide obtained enzymatically from each HS sample is presented in Table 2. A comparison was done with disaccharides derived from a standard commercial bovine kidney HS. Bovine kidney HS showed a similar disaccharide distribution but had a 20% higher degree of sulfation than murine kidney HS. The identities of all disaccharides were confirmed by comparison with standards using HPLC reversed phase ion-pairing analysis [24]. The digestion of the HS samples isolated from different mouse organs, using a mixture of heparin lyases, afforded the same disaccharides found in other previously analyzed vertebrate HS samples, including bovine kidney HS. The major

HS disaccharide, found in whole mouse and all organs, corresponded to UA-GlcNAc and corresponded to 51–73 mole% of the total disaccharides. Interestingly, intestine, followed by lung, in both genders contained the higher percentage of this unsulfated HS disaccharide than previously observed in HS of other mammalian species [9]. The distribution of HS disaccharides in the whole mouse was similar in both genders. Monosulfated disaccharides, UA-GlcNS and UA-GlcNAc6S showed variability (5–16% of total) across different organs but were generally similar between genders. As expected based on previous analyses of bovine kidney HS standard, monosulfated disaccharide, UA2S-GlcNAc, was not detected in any of the samples. The disulfated disaccharide UA-GlcNS6S, while showing some variability (1–8 % of total) across organs, showed the greater intra-gender variation than the other disaccharides, suggesting its utility as gender specificity marker. Disulfated disaccharide, UA2S-GlcNS, showed some variability (4–13%) across organs but little intra-gender differences and was found only in very low levels in intestine. Disulfated disaccharide, UA2S-GlcNAc6S, was higher in the whole animal than might be anticipated from its concentrations in HS obtained from the organs studied. The identity of this relatively rare disaccharide was conformed by co-injection with authentic disulfated disaccharide standard. This suggests that this disaccharide might be rich in organs that were not collected in the current study *e.g.* skeletal muscles that have considerable supply of blood vessels that are highly enriched with endothelial cell lining, bones and the rest of the digestive tract. The UA2S-GlcNS6S disaccharide was at the highest level in female brain. The greatest variability in this study was observed for the trisulfated disaccharide, UA2S-GlcNS6S, commonly found in heparin. Whole animals and many organs, such as eye and kidney, show very low percentages, while HS from other organs, such as liver and brain, show five-fold higher concentration of this disaccharide. Liver HS showed the highest percentage of trisulfated disaccharide (UA2S-GlcNS6S). While this gave murine liver HS a relatively high degree of sulfation of 0.94–0.95, these values were higher than previously reported for mouse liver [13], but considerably lower than other mammalian liver HS (ranging from 1.05–1.21) and much lower than that of the 2.55 value reported for porcine intestinal heparin [8].

### Structural characterization of organs HS using $^1\text{H-NMR}$ spectroscopy

The NMR spectra showed that each HS sample was relatively pure and contained little or no protein, non-HS GAGs or nucleic acid contaminants. Representative 1D spectra are presented (Figures 2–4). 2D-NMR spectroscopy (not shown) allowed the assignment of critical reporter groups in these 1D-NMR spectra. In particular, signals labeled **c**, **e** and **i** at 3.3 ppm, 3.6–3.7 ppm and 4.4 ppm, correspond to individual protons in glucuronic acid, while the signal at 5.1 ppm labeled **j** corresponds to iduronic acid. The spectra of HS clearly demonstrated very low level of iduronic acid content in all HS samples examined [25]. This is an important observation since disaccharide analysis using heparin lyases can not be used to definitively distinguish between glucuronic and iduronic acid. The 3-*O*-sulfo group in glucosamine has a critical function in HS binding to antithrombin and the resulting anticoagulant activity of HS [1]. The 3-*O*-sulfo groups, in glucosamine residues, impart resistance to cleavage heparin lyases [26] making it difficult to determine their presence through disaccharide analysis. While H-NMR spectroscopy show characteristic shifts for the anomeric proton of G1cNS3S residues at 5.5 ppm, no significant signals were observed in

any of the spectra at this position. Finally, the spectra confirm that the GAGs isolated from each tissue were HS and very little, if any, evidence for the presence of heparin could be observed, even in tissues such as lung and intestine, known to be a rich source of pharmaceutical heparins.

## Discussion

Proteomics, measuring gene expression at the protein level, cannot solve questions that arise from post-translational modifications. Glycomics, deals with the study of the structure and function of glycosylated proteins, such as PGs and an understanding of glycome may help explain some unsolved mysteries associated with post-translation modification. The mouse genome is known, so that the study of the glycome of this species represents an important approach for better understanding the role of glycomics in mouse physiology and pathophysiology. HS is regard as one of the most biologically important glycoconjugates and its biosynthesis has been and continues to be extensively studied. Moreover, a recent study has examined the organ developmental specific expression of the enzymes involved in HS biosynthesis in mouse [16].

Functional properties of HS are generally ascribed to its interaction with proteins and often depend on its sulfation pattern and the presence of iduronic acid residues in the polysaccharide [1]. The specificity of protein binding to particular GAG disaccharides is directly related to both the degree of disaccharide sulfation and the position of the sulfate groups, with the 2-*O*-sulfo group in the hexuronic acid residue and the *N*-sulfo and 3-*O* and 6-*O*-sulfo groups in the  $\beta$ -glucosamine residue being major determinants for binding. The presence of flexible iduronic acid residues in most HS samples is also well known to promote heparin interaction with antithrombin III [27,28].

Mice represent an important mammalian organism because their genome is known and experimental powerful array of genetic and molecular tools are available for this model. Knock-out mice have already been prepared that lack enzymes involved in HS biosynthesis, offering the possibility of uncovering the relationship between HS structure and *in vivo* function. However, before the HS structure in knockout animals (usually available in limited numbers and often unavailable as adult animals) can be definitively established, reliable methods need to be developed for isolation, recovery and purification of HS from mouse organs. Moreover, there are no studies suggesting the quantity or structure of murine HS, nor are any systematic studies available of HS quantity and structure across any other mammals. The current study suggest some interesting qualitative and quantitative organ and gender differences in kidney, brain, liver, eye, genitalia and intestine. Some of these organs have been previously shown by our laboratory and others, in a variety of species, to contain HS with distinctive structural features. Many of these distinctive structures are related to physiological and pathophysiological processes. The failure of kidney formation in heparan sulfate 2-*O*-sulfotransferase knock-out mice [29] and defects in the eye and reproductive tract in 3-*O*-sulfotransferase knock-out mice offer important examples [30]. Unfortunately, the disaccharides composition of HS from organs of these knock-out animals has not yet been determined.

The role of HSPG in developmental stage of the embryonal eye [31] and GAG distribution in the different eye part of vertebrates [32] have been described, however, the disaccharide composition of adult vertebrate eye HS not been reported.

Liver HS is believed to act as a receptor for apoE in lipid clearance [33,34]. Our examination of porcine, bovine, and human liver HS [8,35] show that it is rich in highly sulfated sequences and that these are responsible for ApoE interaction [34]. Furthermore, these highly charged liver HS chains also appear to act as receptors for pathogens such as dengue virus [36] and malaria circumsporozoite [37]. It is interesting to note that mice, also sensitive to malaria, have a similar highly sulfated liver HS [38].

Kisilevsky and Szarek [39] found that HS is a critical factor in amyloidogenesis and modifications of sugar precursors of heparan sulfate synthesis that may provide new tool for therapeutic intervention in amyloidogenesis. Study on knock-out mice provided insights of biosynthesis of oversulfated PGs in mice brain [13,40]. Our studies on bovine brain HS showed that it was more highly sulfated than standard bovine kidney HS [41]. Lindahl *et al.* showed that human brain HS was rich in 2-sulfoglucuronic acid [42]. While extensive studies of perlecan proteoglycan protein structure has been made in normal, aged or amyloid deposited Alzheimer's diseased brain [43], disaccharides composition of glycosaminoglycans of normal brain tissues has not been undertaken. The disaccharide analysis of mouse brain also suggests a rich content of 2-sulfouronic acid and a higher sulfation level, again confirming the utility of murine models in studying the brain related diseases of aging. Recent studies have begun to examine the structure [13] of murine brain HS and the activity of HS biosynthetic enzymes [16] within the mouse brain. The current study provides the first gender differences in mouse brain HS.

In conclusion, HS is found at different concentrations and structures throughout the body of mice. While all murine HS analyzed was relatively low in degree of sulfation [44] some slight gender specific as well as organ specific differences in murine HS was observed. Future studies are planned to immobilize the HS prepared onto surface plasmon resonance biochips. SPR will then be used to examine binding kinetics ( $k_{on}$  and  $k_{off}$ ) of HS isolated from various mouse organs with different heparin-binding proteins (growth factors, chemokines, virus envelope proteins, *etc.*) [45]. In addition, future studies will examine the application of microdissection techniques to separate organs into different tissue and/or cell population types for HS extraction and disaccharide analysis characterization. These studies represent an initial approach to structural glycomics and suggest a need for additional studies in functional glycomics of glycan structures of HS to explain phenotypes (or the lack thereof) in knock-out mice. Tissues from knock-out mice are currently in collected for similar analysis. With the mouse genome established and proteomics under intensive investigation, these post-translation modifications and the glycome represent the next frontier in understanding many unsolved mysteries in cellular as well as extracellular biology.

## Acknowledgments

This research was supported by grants GM38060, HL52622 and HL6244 from the National Institutes of Health.

## Abbreviations

|                      |   |
|----------------------|---|
| <b>GAGs</b>          | glycosaminoglycans  |
| <b>PG</b>            | proteoglycans   |
| <b>HS</b>            | heparan sulfate   |
| <b>SPR</b>           | surface plasmon resonance   |
| <b>MWCO</b>          | molecular weight cut-off  |
| <b>UA-GlcNAc</b>     | 2-acetamido-2-deoxy-4- <i>O</i> -(4-deoxy- $\alpha$ -L- <i>threo</i> -hexenopyranosyluronic acid)-D-glucose                                       |
| <b>UA-GlcNS</b>      | 2-deoxy-2-sulfamido-4- <i>O</i> -(4-deoxy- $\alpha$ -L- <i>threo</i> -hexenopyranosyluronic acid)-D-glucose                                       |
| <b>UA-GlcNAc6S</b>   | 2-acetamido-2-deoxy-4- <i>O</i> -(4-deoxy- $\alpha$ -L- <i>threo</i> -hexenopyranosyluronic acid)-6- <i>O</i> -sulfo-D-glucose                    |
| <b>UA2S-GlcNAc</b>   | 2-acetamido-2-deoxy-4- <i>O</i> -(4-deoxy-2- <i>O</i> -sulfo- $\alpha$ -L- <i>threo</i> -hexenopyranosyluronic acid)-D-glucose                    |
| <b>UA-GlcNS6S</b>    | 2-deoxy-2-sulfamido-4- <i>O</i> -(4-deoxy-2- <i>O</i> -sulfo- $\alpha$ -L- <i>threo</i> -hexenopyranosyluronic acid)-6- <i>O</i> -sulfo-D-glucose |
| <b>UA2S-GlcNS</b>    | 2-deoxy-2-sulfamido-4- <i>O</i> -(4-deoxy-2- <i>O</i> -sulfo- $\alpha$ -L- <i>threo</i> -hexenopyranosyluronic acid)-D-glucose                    |
| <b>UA2S-GlcNAc6S</b> | 2-acetamido-2-deoxy-4- <i>O</i> -(4-deoxy-2- <i>O</i> -sulfo- $\alpha$ -L- <i>threo</i> -hexenopyranosyluronic acid)-6- <i>O</i> -sulfo-D-glucose |
| <b>UA2S-GlcNS6S</b>  | 2-deoxy-2-sulfamido-4- <i>O</i> -(4-deoxy-2- <i>O</i> -sulfo- $\alpha$ -L- <i>threo</i> -hexenopyranosyluronic acid)-6- <i>O</i> -sulfo-D-glucose |
| <b>CPC</b>           | cetylpyridinium chloride  |
| <b>COSY</b>          | correlation spectroscopy  |

## References

1. Capila I, Linhardt RJ. Heparin – protein interactions. *Angew. Chemie. Int. Ed.* 2002; 41:390–412.
2. Gomes PB, Dietrich CP. Distribution of heparin and other sulfated glycosaminoglycans in vertebrates. *Compar. Biochem. Physiol.* 1982; 73:857–863.
3. Dietrich CP, Nader HB, Straus AH. Structural differences of heparan sulfates according to the tissue and species of origin. *Biochem. Biophys. Res. Commun.* 1983; 111:865–871. [PubMed: 6220714]
4. Medeiros GF, Mendes A, Castro RA, Bau EC, Nader HB, Dietrich CP. Distribution of sulfated glycosaminoglycans in the animal kingdom: widespread occurrence of heparin-like compounds in invertebrates. *Biochim. Biophys. Acta.* 2000; 1475:287–294. [PubMed: 10913828]
5. Toyoda H, Kinoshita-Toyoda A, Selleck S. Structural analysis of glycosaminoglycans in *Drosophila* and *Caenorhabditis elegans* and demonstration that tout-velu, a *Drosophila* gene related to EXT tumor suppressors, affects heparan sulfate in vivo. *J. Biol. Chem.* 2000; 275:2269–2275. [PubMed: 10644674]
6. Turnbull J, Drummond K, Huang Z, Kinnunen T, Ford-Perriss M, Murphy M, Guimond S. Heparan sulphate sulphotransferase expression in mice and *Caenorhabditis elegans*. *Biochem. Soc. Trans.* 2003; 31:343–348. [PubMed: 12653634]

7. Warda M, Mao W, Toida T, Linhardt RJ. Turkey intestine as a commercial source of heparin? Comparative structural studies of intestinal avian and mammalian glycosaminoglycans. *Comp. Biochem. Physiol. B.* 2003; 134:189–197. [PubMed: 12524047]
8. Vongchan P, Warda M, Toyoda H, Toida T, Marks RM, Linhardt RJ. Structural characterization of human liver heparan sulfate. *Biochim. Biophys. Acta.* 2005; 1721:1–8. [PubMed: 15652173]
9. Warda M, Linhardt RJ. Dromedary glycosaminoglycans: Molecular characterization of camel lung and liver heparan sulfate. *Comp. Biochem. Phys. B.* 2006; 143:37–43.
10. Warda M, Gouda EM, Toida T, Chi L, Linhardt RJ. Isolation and characterization of raw heparin from dromedary intestine: evaluation of a new source of pharmaceutical heparin. *Comp. Biochem. Physiol. C.* 2003; 136:357–365.
11. Maccarana M, Sakura Y, Tawada A, Yoshida K, Lindahl U. Domain structure of heparan sulfates from bovine origin. *J. Biol. Chem.* 1996; 271:17804–17810. [PubMed: 8663266]
12. Lindahl B, Lindahl U. Amyloid-specific heparan sulfate from human liver and spleen. *J. Biol. Chem.* 1997; 272:26091–26094. [PubMed: 9334172]
13. Ledin J, Staatz W, Li J-P, Götte M, Selleck S, Kjellén L, Spillmann D. Heparan sulfate structure in mice with genetically modified heparan sulfate production. *J. Biol. Chem.* 2004; 279:42732–42741. [PubMed: 15292174]
14. Rykova VI, Grigorieva EV. Proteoglycan composition in cell nuclei of mouse hepatoma. *Biochem.* 1998; 63:1271–1276. [PubMed: 9864465]
15. Esko JD, Selleck SB. Order out of chaos: assembly of ligand binding sites in heparan sulfate. *Ann. Rev. Biochem.* 2002; 71:435–471. [PubMed: 12045103]
16. Yabe T, Hata T, He J, Maeda N. Developmental and regional expression of heparan sulfate sulfotransferase genes in the mouse brain. *Glycobiol.* 2005; 15:982–993.
17. Razi N, Lindahl U. Biosynthesis of heparin/heparan sulfate. The d-glucosaminyl 3-*O*-sulfotransferase reaction: target and inhibitor saccharides. *J. Biol. Chem.* 1995; 270:11267–11275. [PubMed: 7744762]
18. Gallagher JT, Turnbull JE, Lyon M. Patterns of sulphation in heparan sulfate: Polymorphism based on a common structural theme. *Int. J. Biochem.* 1992; 24:553–560. [PubMed: 1516727]
19. Liu J, Shworak NW, Sinaÿ P, Schwartz JJ, Zhang L, Fritze LMS, Rosenberg RD. Expression of heparan sulfate d-Glucosaminyl 3-*O*-Sulfotransferase isoforms reveals novel substrate specificities. *J Biol. Chem.* 1999; 274:5185–5192. [PubMed: 9988768]
20. Heinegard D, Sommarin Y. Isolation and characterization of proteoglycans. *Meth. Enzymol.* 1987; 144:319–372. [PubMed: 3626874]
21. Furukawa K, Terayama H. Isolation and identification of glycosaminoglycans associated with purified nuclei from rat liver. *Biochim. Biophys. Acta.* 1977; 499:278–289. [PubMed: 907787]
22. Griffin CC, Linhardt RJ, Van Gorp CL, Toida T, Hileman RE, Schubert RL, Brown SE. Isolation and characterization of heparan sulfate from crude porcine intestinal mucosa peptidoglycan heparin. *Carbohydr. Res.* 1995; 276:183–197. [PubMed: 8536254]
23. Toyoda H, Kinoshita-Toyoda A, Selleck S. Structural analysis of glycosaminoglycans in *Drosophila* and *Caenorhabditis elegans* and demonstration that tout-velu, a *Drosophila* gene related to EXT tumor suppressors, affects heparan sulfate in vivo. *J. Biol. Chem.* 2000; 275:2269–2275. [PubMed: 10644674]
24. Imanari T, Toida T, Koshiishi I, Toyoda H. High-performance liquid chromatographic analysis of glycosaminoglycan-derived oligosaccharides. *J. Chromatogr. A.* 1996; 720:275–293. [PubMed: 8601196]
25. Sudo M, Sato K, Chaidedgumjorn A, Toyoda H, Toida T, Imanari T. <sup>1</sup>H nuclear magnetic resonance spectroscopic analysis for determination of glucuronic and iduronic acids in dermatan sulfate, heparin, and heparan sulfate. *Anal. Biochem.* 2001; 297:42–51. [PubMed: 11567526]
26. Yu G, LeBrun L, Gunay NS, Hoppensteadt D, Walenga J, Fareed J, Linhardt RJ. Heparinase I acts on a synthetic heparin pentasaccharide corresponding to the antithrombin III binding site. *Thromb. Res.* 2000; 100:549–556. [PubMed: 11152935]
27. Lei PS, Duchaussoy P, Sizun P, Mallet JM, Petitou M, Sinaÿ P. Synthesis of a 3-deoxy-l-iduronic acid containing heparin pentasaccharide to probe the conformation of the antithrombin III binding sequence. *Bioorg. Med. Chem.* 1998; 6:1337–1346. [PubMed: 9784873]

28. Desai UR, Petitou M, Bjork I, Olson ST. Mechanism of heparin activation of antithrombin: evidence for an induced-fit model of allosteric activation involving two interaction subsites. *Biochem.* 1998; 37:13033–13041. [PubMed: 9737884]
29. Bullock SL, Fletcher JM, Beddington RS, Wilson VA. Renal agenesis in mice homozygous for a gene trap mutation in the gene encoding heparan sulfate 2-sulfotransferase. *Genes & Developm.* 1998; 12:1894–1906.
30. HajMohammadi S, Enjoji K, Princiville M, Christi P, Lech M, Beeler DL, Rayburn H, Schwartz JJ, Barzegar S, de Agostini AI, Post MJ, Rosenberg RD, Shworak NW. Normal levels of anticoagulant heparan sulfate are not essential for normal hemostasis. *J. Clin. Invest.* 2003; 111:989–999. [PubMed: 12671048]
31. Araki M, Takano T, Uemonsa T, Nakane Y, Tsudzuki M, Kaneko T. Epithelia-mesenchyme interaction plays an essential role in transdifferentiation of retinal pigment epithelium of silver mutant quail: localization of FGF and related molecules and aberrant migration pattern of neural crest cells during eye rudiment formation. *Developm. Biol.* 2002; 244:358–371.
32. Goes RM, Laicine EM, Porcionatto MA, Bonciani Nader H, Haddad A. Glycosaminoglycans in components of the rabbit eye: synthesis and characterization. *Current Eye Res.* 1999; 19:146–153.
33. Auger A, Truong TQ, Rhainds D, Lapointe J, Letarte F, Brissette L. Low and high density lipoprotein metabolism in primary cultures of hepatic cells from normal and apolipoprotein E knockout mice. *Eur. J. Biochem.* 2001; 268:2322–2330. [PubMed: 11298750]
34. Libeu CP, Lund-Katz S, Phillips MC, Wehrli S, Hernaiz MJ, Capila I, Linhardt RJ, Raffai RL, Newhouse YM, Zhou F, Weisgraber KH. New insights into the heparan sulfate proteoglycan-binding activity of apolipoprotein. *EJ. Biol. Chem.* 2001; 276:39138–39144.
35. Hernaz MJ, Yang HO, Gunay NS, Linhardt RJ. Purification and Characterization of Heparan Sulfate Peptidoglycans from Bovine Liver. *Carbohydr. Polym.* 2002; 48:153–160.
36. Chen Y, Maguire T, Hileman RE, Fromm JR, Esko JD, Linhardt RJ, Marks RM. Dengue Virus Infectivity Depends on Envelope Protein Binding to Target Cell Heparan Sulfate. *Nat. Med.* 1997; 3:866–871. [PubMed: 9256277]
37. Rathore D, McCutchan TF, Hernaz MJ, LeBrun LA, Lang SC, Linhardt RJ. Direct Measurement of the Interaction of Glycosaminoglycans and a Heparin Decasaccharide with Malaria Circumsporozoite Protein. *Biochemistry.* 2001; 40:11518–11524. [PubMed: 11560500]
38. Rathore D, Hrstka SCL, Sacci JB, de la Vega P, Linhardt RJ, Kumar S, McCutchan TF. Molecular Mechanism of Host Specificity in Plasmodium falciparum Infection: Role of Circumsporozoite Protein. *J. Biol. Chem.* 2003; 278:40905–40910. [PubMed: 12904297]
39. Kisilevsky R, Szarek WA. Novel glycosaminoglycan precursors as anti-amyloid agents part II. *J. Molec. Neurosci.* 2002; 19:45–50. [PubMed: 12212792]
40. Uchimura K, Kadomatsu K, Nishimura H, Muramatsu H, Nakamura E, Kurosawa N, Habuchi O, El-Fasakhany FM, Yoshikai Y, Muramatsu T. Functional analysis of the chondroitin 6-sulfotransferase gene in relation to lymphocyte subpopulations, brain development, and oversulfated chondroitin sulfates. *Biol. Chem.* 2002; 277:1443–1450.
41. Park Y, Yu G, Gunay NS, Linhardt RJ. Purification and Characterization of Heparan Sulphate Proteoglycan from Bovine Brain. *Biochem. J.* 1999; 344:723–730. [PubMed: 10585858]
42. Kinnunen T, Raulo E, Nolo R, Maccarana M, Lindahl U, Rauvala H. Neurite outgrowth in brain neurons induced by heparin-binding growth-associated molecule (HB-GAM) depends on the specific interaction of HB-GAM with heparan sulfate at the cell surface. *J. Biol. Chem.* 1996; 271:2243–2248. [PubMed: 8567685]
43. Maresh GA, Erezylmaz D, Murry CE, Nochlin D, Snow AD. Detection and quantitation of perlecan mRNA levels in Alzheimer’s disease and normal aged hippocampus by competitive reverse transcription-polymerase chain reaction. *J. Neurochem.* 1996; 67:1132–1144. [PubMed: 8752120]
44. Toida T, Yoshida H, Toyoda H, Koshiishi I, Imanari T, Hileman RE, Fromm JR, Linhardt RJ. Structural differences and the presence of unsubstituted amino groups in heparan sulphates from different tissues and species. *Biochem. J.* 1997; 322:499–506. [PubMed: 9065769]
45. Linhardt RJ, Toida T. Role of Glycosaminoglycans in Cellular Communication. *Acc. Chem. Res.* 2004; 37:431–438. [PubMed: 15260505]

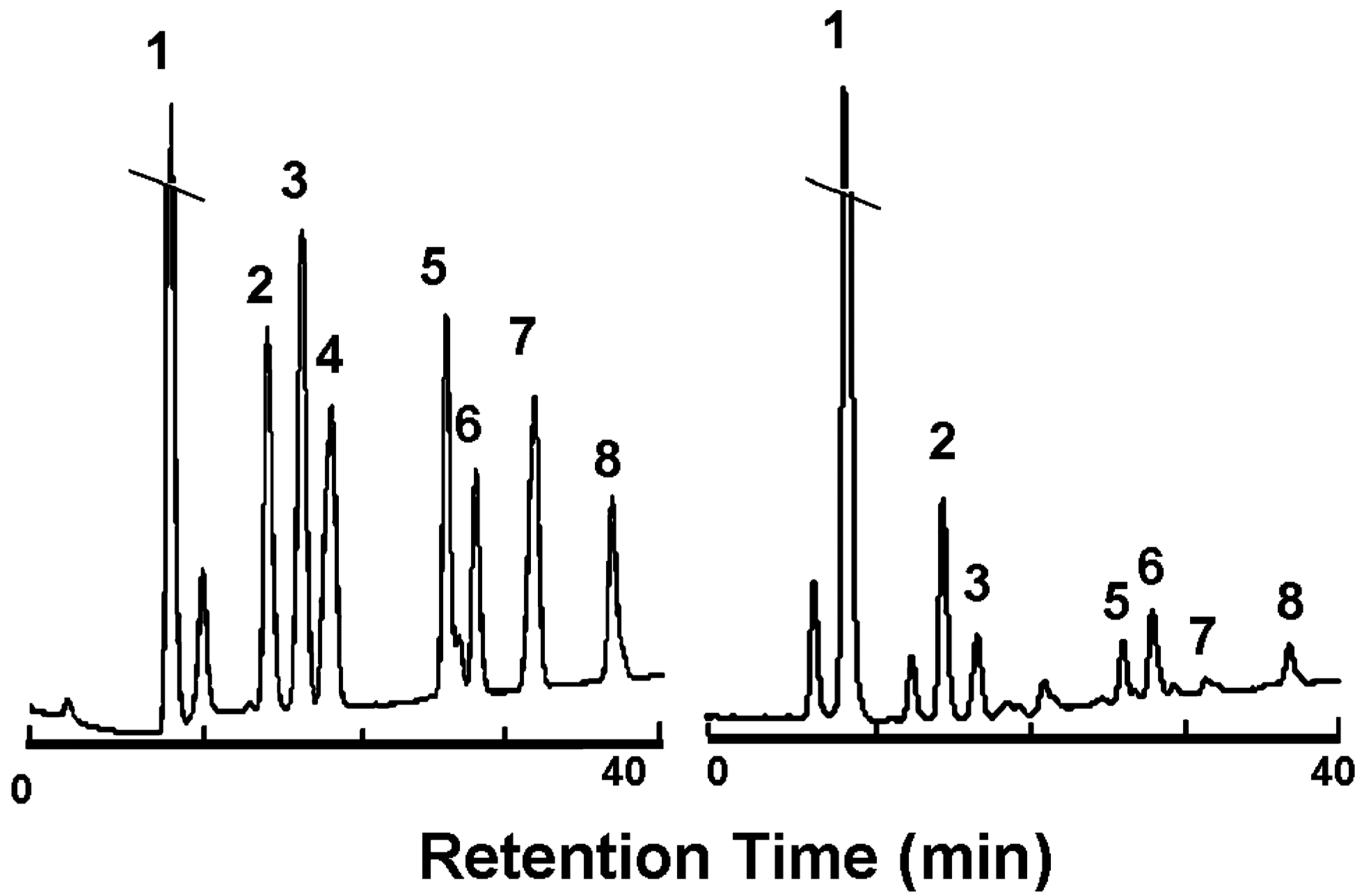


**Fig. 1.** HPLC disaccharide analysis. Eight disaccharide standards (1–8, see Table 2) are analyzed in left panel and extracted female mouse lung HS is analyzed in the right panel.

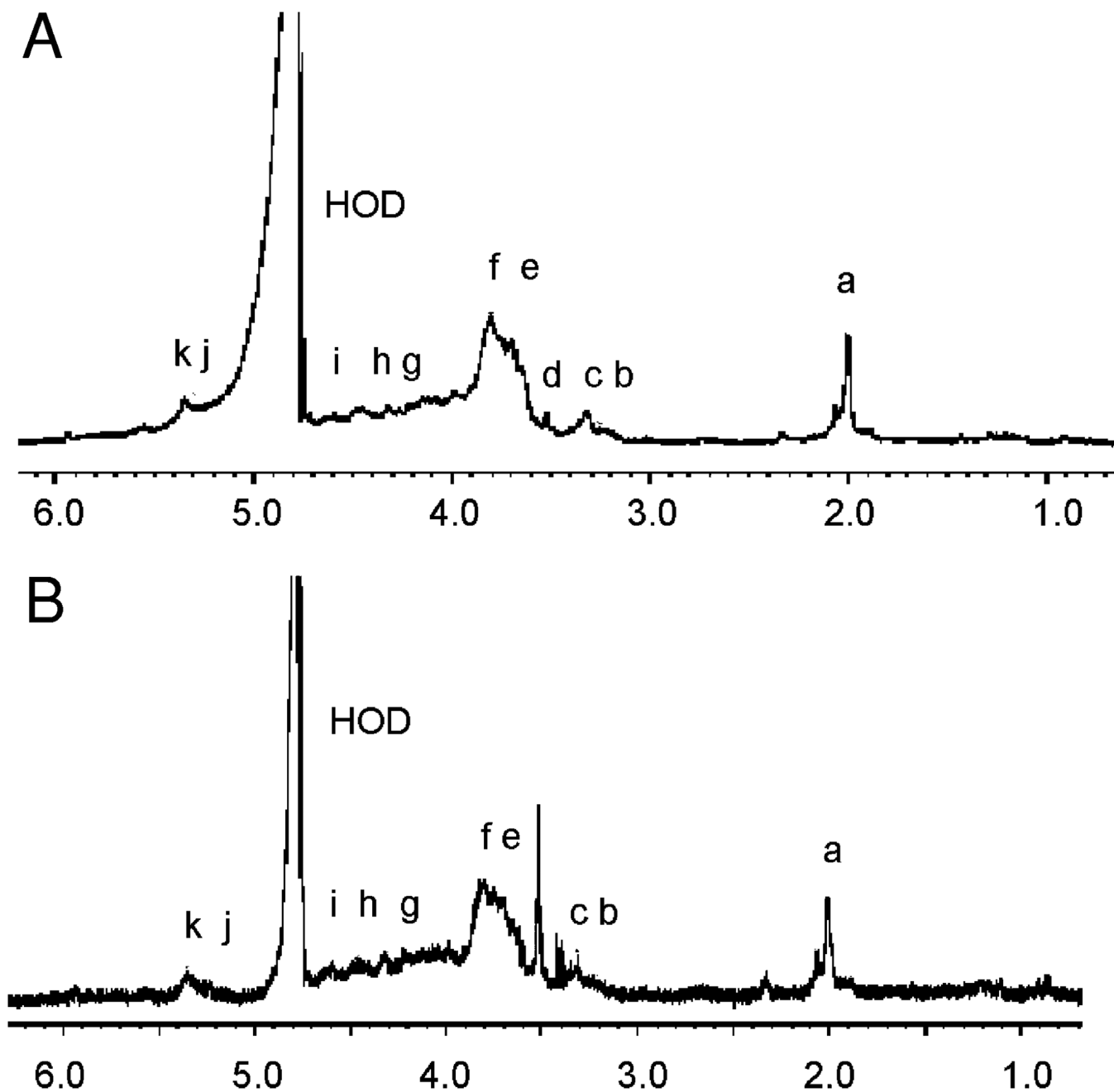


**Fig. 2.**

<sup>1</sup>H-NMR spectra of HS from whole male mice (A) and whole female mice (B). Reporter signals correspond to **a.** *N*-acetyl (CH<sub>3</sub>) GlcNAc (2.0 ppm); **b.** GlcNS, H-2 (3.2 ppm); **c.** GlcA, H-2 (3.3 ppm); **d.** GlcNS and GlcA, H-3 (3.5 ppm); **e.** GlcA, H-4 and H-5 (3.6–3.7 ppm); **f.** GlcNAc, H-2 (3.8 ppm); **g.** IdoA2S H-3 and GlcNS6S, H6a (4.2 ppm); **h.** IdoA2S, H-2 and GlcNS6S, H-6b (4.3 ppm); **i.** GlcA, H-1 (4.4 ppm); **j.** IdoA, H-1 (5.1 ppm); and **k.** GlcN (Ac or S) H-1 (5.4 ppm).

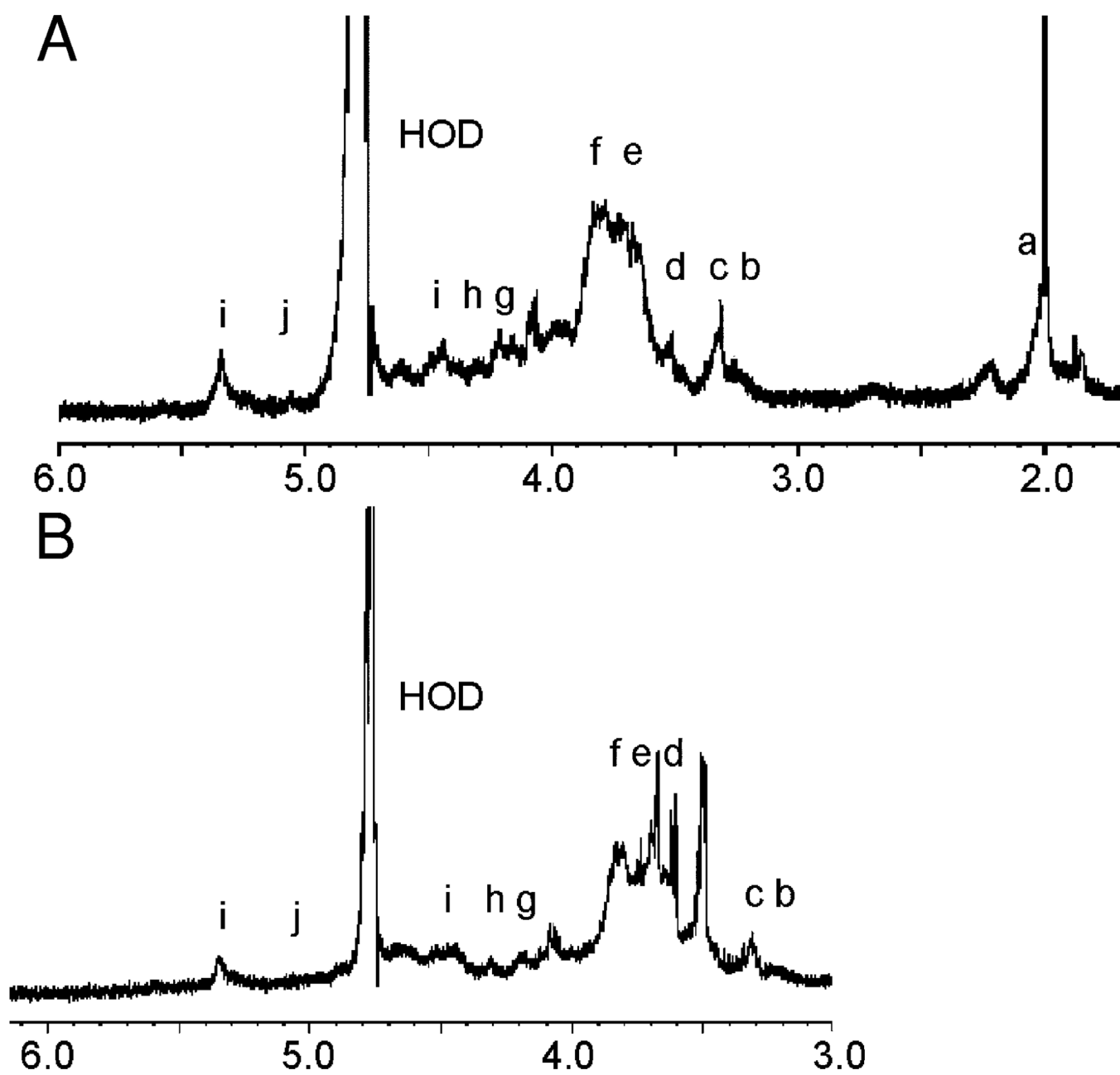


**Fig. 3.**  $^1\text{H-NMR}$  spectra of HS from male mouse kidney (**A**) and female mouse kidney (**B**). Reporter signals labeled **a–k** are as assigned in Figure 2.

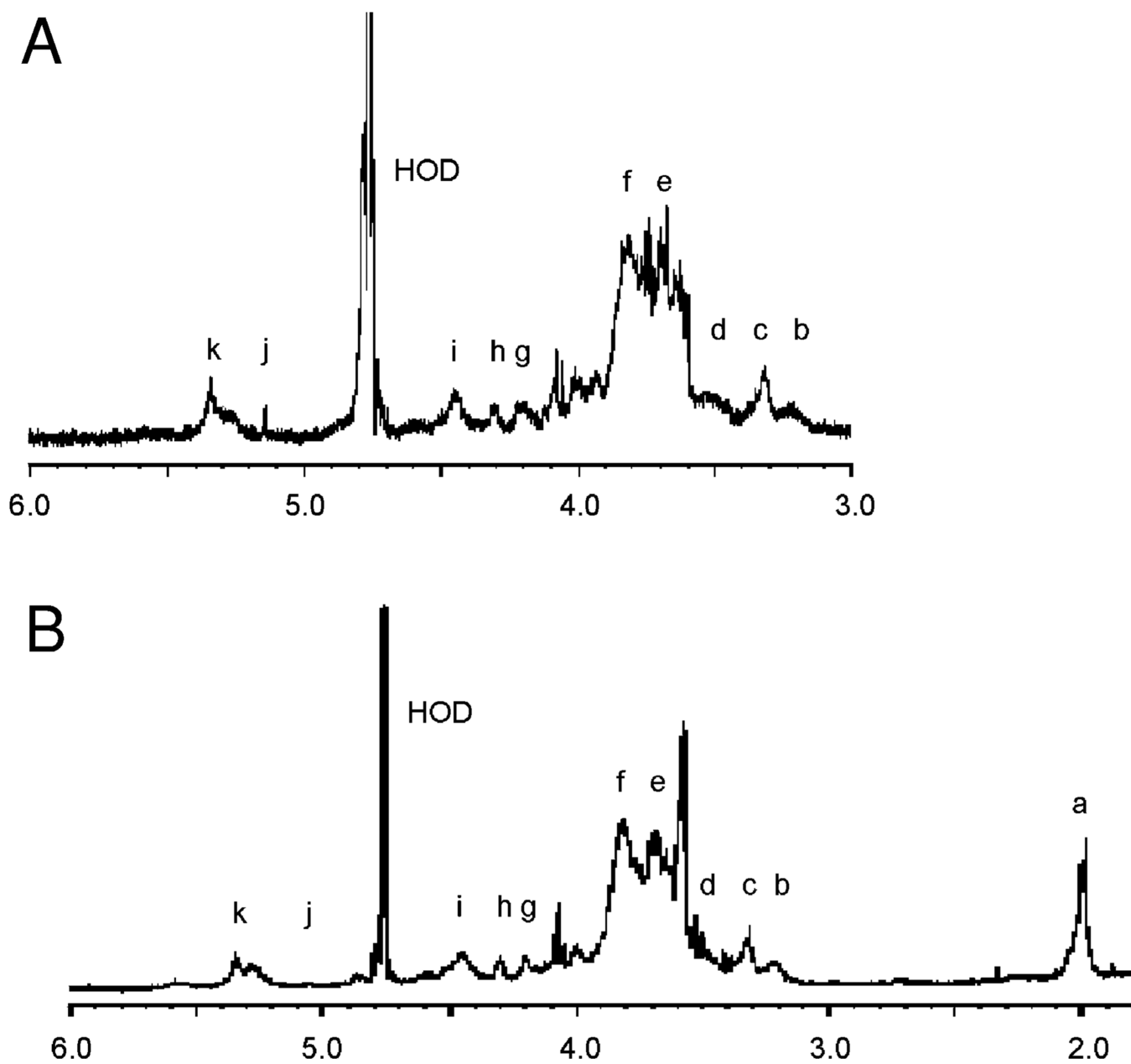


**Fig. 4.**  $^1\text{H-NMR}$  spectra of HS from male mouse lung (**A**) and female mouse lung (**B**). Reporter signals labeled **a–k** are as assigned in Figure 2.

**Table 1**

Organ distribution of HS in ICR strain mice (6–8 week)

|                                | Whole animal | Liver | Lung  | Heart | Kidney | Brain | Spleen            | Intestine | Skin | Eye   |
|--------------------------------|--------------|-------|-------|-------|--------|-------|-------------------|-----------|------|-------|
| Male                           |              |       |       |       |        |       |                   |           |      |       |
| Fresh wet wt. of tissue (g)    | 33.5         | 2.24  | 0.26  | 0.15  | 0.64   | 0.43  | 0.12              | 2.78      | 3.75 | 0.04  |
| Defatted dry wt. of tissue (g) | 7.33         | 0.5   | 0.05  | 0.03  | 0.11   | 0.05  | 0.028             | 0.41      | 1.34 | 0.008 |
| Total HS (mg)                  | 0.89         | 0.06  | 0.037 | 0.025 | 0.018  | 0.165 | n.d. <sup>a</sup> | 0.22      | 0.30 | 0.007 |
| Female                         |              |       |       |       |        |       |                   |           |      |       |
| Fresh wet wt. of tissue (g)    | 24.6         | 1.65  | 0.24  | 0.124 | 0.39   | 0.46  | 0.106             | 2.49      | 2.76 | 0.04  |
| Defatted dry wt. of tissue (g) | 5.45         | 0.32  | 0.04  | 0.021 | 0.056  | 0.058 | 0.017             | 0.39      | 0.58 | 0.006 |
| Total HS (mg)                  | 0.67         | 0.19  | 0.03  | 0.017 | 0.037  | 0.055 | 0.027             | 0.18      | 0.21 | 0.002 |

<sup>a</sup> not determined.

Table 2

## Disaccharide composition of HS

|           | UA-GlcNAc | UA-GlcNS | UA-GlcNAc6S | UA-GlcNAc         | UA-GlcNS6S | UA2S-GlcNS | UA2S-GlcNAc6S | UA2S-GlcNS | UA2S-GlcNAc6S | UA2S-GlcNS6S | Deg. Of Sulfation <sup>a</sup> |
|-----------|-----------|----------|-------------|-------------------|------------|------------|---------------|------------|---------------|--------------|--------------------------------|
| mouse, m  | 59.4      | 8.2      | 10.4        | n.d. <sup>b</sup> | 6.8        | 8.5        | 5.2           | 8.5        | 5.2           | 1.5          | 0.64                           |
| liver     | 50.9      | 10.2     | 12.4        | n.d.              | 5.1        | 4.4        | <0.5          | 4.4        | <0.5          | 17.0         | 0.94                           |
| lung      | 63.5      | 12.2     | 2.1         | n.d.              | 4.6        | 6.8        | 1.4           | 6.8        | 1.4           | 9.4          | 0.64                           |
| kidney    | 60.4      | 14.4     | 10.8        | n.d.              | 4.4        | 6.2        | 2.5           | 6.2        | 2.5           | 1.3          | 0.55                           |
| brain     | 50.2      | 7.7      | 7.9         | n.d.              | 7.3        | 11.7       | 3.1           | 11.7       | 3.1           | 12.1         | 0.96                           |
| eye       | 56.1      | 15.5     | 12.8        | n.d.              | 4.4        | 7.3        | 2.4           | 7.3        | 2.4           | 1.5          | 0.61                           |
| intestine | 72.8      | 14.8     | 4.2         | n.d.              | 1.2        | 1.4        | 1.2           | 1.4        | 1.2           | 4.4          | 0.40                           |
| skin      | 61.4      | 13.4     | 9.3         | n.d.              | 6.5        | 4.8        | 2.4           | 4.8        | 2.4           | 2.2          | 0.57                           |
| mouse, f  | 60.2      | 7.5      | 12.2        | n.d.              | 6.8        | 7.2        | 4.4           | 7.2        | 4.4           | 1.5          | 0.61                           |
| liver     | 52.0      | 12.0     | 8.4         | n.d.              | 8.2        | 4.0        | 1.2           | 4.0        | 1.2           | 15.9         | 0.95                           |
| lung      | 66.2      | 10.2     | 3.4         | n.d.              | 6.5        | 6.0        | 2.0           | 6.0        | 2.0           | 7.6          | 0.65                           |
| heart     | 58.6      | 14.4     | 8.6         | n.d.              | 4.6        | 4.2        | 2.0           | 4.2        | 2.0           | 7.6          | 0.67                           |
| kidney    | 60.4      | 13.8     | 9.2         | n.d.              | 1.8        | 5.0        | 1.5           | 5.0        | 1.5           | 1.9          | 0.45                           |
| brain     | 52.2      | 5.7      | 6.0         | n.d.              | 7.0        | 13.0       | 4.5           | 13.0       | 4.5           | 10.4         | 0.80                           |
| eye       | 55.5      | 16.5     | 12.2        | n.d.              | 8.2        | 6.6        | 2.6           | 6.6        | 2.6           | 2.0          | 0.69                           |
| intestine | 70.6      | 16.6     | 4.8         | n.d.              | 4.6        | 1.6        | 1.2           | 1.6        | 1.2           | 3.4          | 0.46                           |
| skin      | 62.0      | 12.2     | 8.5         | n.d.              | 4.6        | 6.6        | 1.5           | 6.6        | 1.5           | 2.6          | 0.54                           |
| spleen    | 64.0      | 11.6     | 8.0         | n.d.              | 6.6        | 6.8        | 2.2           | 6.8        | 2.2           | 2.6          | 0.59                           |
| kidney    | 56.4      | 15.9     | 12.8        | n.d.              | 4.2        | 7.2        | 2.2           | 7.2        | 2.2           | 1.3          | 0.60                           |

<sup>a</sup> Degree of sulfation is the average number of sulfo groups/disaccharide calculated from the disaccharide analysis.

<sup>b</sup> Values expressed in mole %.